Inorg. Chem. **2004**, *43*, 6203–6214

Mononuclear, Five-Coordinate Lanthanide Amido and Aryloxide Complexes Bearing Tetradentate (N_2O_2) Schiff Bases

Steven A. Schuetz,[†] Carter M. Silvernail,[†] Christopher D. Incarvito,[‡] Arnold L. Rheingold,[‡] Joanna L. Clark,[†] Victor W. Day,[†] and John A. Belot*,[†]

Department of Chemistry and the Center for Materials Research and Analysis, University of Nebraska, Lincoln, Nebraska 68588, and Department of Chemistry and Biochemistry, University of Delaware, Newark, Delaware 19716

Received January 21, 2004

Two monomeric, five-coordinate lanthanide complexes, [bis-5,5′-(1,3-propanediyldiimino)-2,2-dimethyl-4-hexene-3-onato]samarium[2,6-bis(*tert*-butyl)-4-methylphenoxide] and [bis-5,5′-(1,3-propanediyldiimino)-2,2-dimethyl-4-hexene-3-onato]erbium[2,6-bis(*tert*-butyl)-4-methylphenoxide], were isolated from the reactions of 2,6-bis(*tert*-butyl)-4-methylphenol with [bis-5,5′-(1,3-propanediyldiimino)-2,2-dimethyl-4-hexene-3-onato]lanthanide[bis(trimethylsilyl)amido] (lanthanide = Er^{3+} and Sm^{3+}). The purified phenoxides were recovered in excellent yields and analytical purity, and the reactions proceeded cleanly without Schiff-base degradation or cluster formation. Analogously, [bis-3,3′-(1,3-propanediyldiimino)-1-phenyl-2-butene-1-onato]erbium[bis(trimethylsilyl)amido] was also directly converted to [bis-3,3′-(1,3-propanediyldiimino)-1-phenyl-2-butene-1-onato]erbium[2,6-bis(*tert*-butyl)-4-methylphenoxide]; however, a less sterically demanding alcohol (i.e., ethanol) yielded a neutral trinuclear oxo alkoxide species with each dianionic Schiff base asymmetrically bridging through μ-oxo interactions. In this polynuclear cluster, each symmetry-related, seven-coordinate erbium(III) ion exhibits monocapped trigonal prismatic geometry, which assembles by sharing triangular capped faces. Single-crystal X-ray diffraction revealed square-pyramidal metal coordination in each five-coordinate lanthanide ion with varied S_4 ruffling of the "square base" donor atoms and the six-membered propylene diamine chelate ring adopting the boat conformation. To contrast the effect of subtle ligand changes, we also report the synthesis and characterization of [bis-5,5′-(2,2-dimethyl-1,3-propanediyldiimino)-2,2-dimethyl-4-hexene-3-onato]samarium[bis(trimethylsilyl)amido], having *gem*-dimethyl substituents appended to the propylene bridge central carbon. The six-membered diamine chelate ring in this compound adopts the chair conformation without metal–hydrocarbon interaction. Also presented are qualitative activity observations and polymerization data for the polymerization of *rac*-lactide and ϵ-caprolactone using the five-coordinate lanthanide amidos and phenoxides.

Introduction

A common theme in contemporary f-element chemistry is identifying alternative ligand scaffolds beyond cyclopentadienyl-based coordination environments that maintain the low coordination numbers and catalytic activity of organometallic Ln^{3+} complexes.[1a−e] Toward this goal, various anhydrous, hard donor-atom (i.e., N or O) frameworks have been the subject of recent investigations; relevant examples include heteroleptic guanidinates,[2a,b] calix[4]arenes,[3] porphyrins,[4] β-diketiminato,[5] and tetradentate Schiff bases.[6a−k] Of these potential organic scaffolds, the latter offer the distinct advantages of ease of synthesis, low cost, rapid tailorability at both peripheral and prochiral backbone sites,

* Author to whom correspondence should be addressed. E-mail: jbelot2@unl.edu.

[†] University of Nebraska−Lincoln.

[‡] University of Delaware. Present address: Departments of Chemistry and Biochemistry, University of California−San Diego, La Jolla, CA 92093.

(1) (a) Dehnicke, K.; Greiner, A. *Angew. Chem., Int. Ed.* **2003**, *42*, 1340. (b) Piers, W. E.; Emslie, J. J. H. *Coord. Chem. Rev.* **2002**, *233−234*, 131. (c) Aspinall, H. C. *Chem. Rev.* **2002**, *102*, 1807. (d) Roesky, P. W. *Chem. Soc. Rev.* **2000**, *29*, 335. (e) Evans, W. J. *New J. Chem.* **1995**, *19*. 525.

(2) (a) Giesbrecht, G. R.; Whitener, G. D.; Arnold, J. *J. Chem. Soc., Dalton Trans.* **2001**, 923. (b) Noss, H.; Oberthür, M.; Fischer, C.; Kretschmer, W. P.; Kempe, R. *Eur. J. Inorg. Chem.* **1999**, 2283.

(3) Estler, F.; Herdtweck, E.; Anwander, R. *J. Chem. Soc., Dalton Trans.* **2002**, 3088.

(4) Foley, T. J.; Abboud, K. A.; Boncella, J. M. *Inorg. Chem.* **2002**, *41*, 1704.

(5) Neculai, A. M.; Roesky, H. W.; Neculai, D.; Magull, J. *Organometallics* **2001**, *20*, 5501.

10.1021/ic040006f CCC: $27.50
Published on Web 09/04/2004

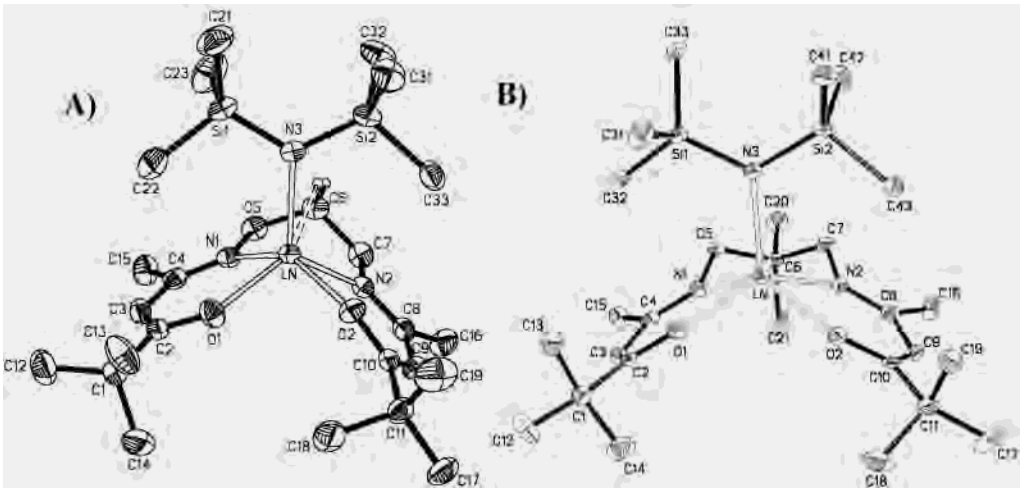

Figure 1. General diffraction-derived structures of mononuclear amino complexes containing methylene (A) and *gem*-dimethyl (B) substituents along the pseudomolecular mirror plane.

and ample literature precedent.[7] However, isolating low coordination number, anhydrous, f-element complexes bearing these ligands is fraught with obstacles and undoubtedly contributes to the paucity of literature reports.[1b,c] For example, anhydrous Salen-based lanthanide complexes often utilize high coordination numbers (>6) via dinuclear Ln_2L_3 formation (L = tetradentate Salen), whose formation is believed to be enhanced by π stacking.[8a−b] Lewis base solvent stabilization of the coordinately unsaturated metal center also presents higher coordination number ions[6a] but stabilizes mononuclear Salen complexes containing group III elements.[6d,9a,b] Regarding the latter, Evans[6d] reported a variety of solvated Y^{3+} Salen-based compounds that are particularly germane to this study.

The importance of synthesizing mononuclear lanthanide complexes and understanding the conditions required to promote their formation is that the complexes can be utilized as catalysts for small molecules and the polymerization of polar molecules (vide infra). With the new, readily available, low-cost, easily tailored lanthanide Schiff-base catalysts described herein, there is seemingly unlimited potential to tailor ligands at multiple sites as well as metal apical substituents to enable small-molecule transformations exploiting f-element attributes. We previously reported the synthesis and characterization of mononuclear Sm^{3+} (**1**)[6e] and Er^{3+} (**2**) amido complexes bearing "saturated" Schiff bases (Figure 1A and B, respectively) as well as the stoichiometric hydrolysis chemistry of the mononuclear erbium amido, **2**.[6c] Inspired by the subtle structural differences within these molecules and the significant amido lability, we began to evaluate alternative substitution patterns on the Schiff-base (SB) periphery as well as the direct replacement of the bulky bis(trimethylsilyl)amido group using various Brønsted acids. Specifically, we sought to yield more accessible rare-earth ions for a variety of substrates by decreasing ketoiminato (KI) frontal steric bulk through ^{t}Bu group replacement. We also postulated increased axial-ligand nucleophilicity toward incoming substrates in mononuclear (KI)Ln(alkoxide) species. Although the ability to tailor Schiff bases is the crux of their desirability,[1c,7] identifying the lower limit of steric bulk required to recover stable mononuclear species successfully for small charge-to-radius ratio ions remains challenging. Furthermore, we sought to establish that the mononuclear amido complexes would undergo ligand exchange reactions without ketoiminato degradation, replacement, or protonolysis by alcohols,[5] thereby proving themselves to be versatile, stable platforms for future work involving the polymerization of cyclic ester or epoxide monomers or small-molecule transformations.

Herein, we present the results of stoichiometric reactions between alcohols and three unique rare-earth Schiff-base amido complexes, [bis-5,5′-(1,3-propanediyldiimino)-2,2-dimethyl-4-hexene-3-onato]samarium[bis(trimethylsilyl)amido] (**1**), [bis-5,5′-(1,3-propanediyldiimino)-2,2-dimethyl-4-hexene-3-onato]erbium[bis(trimethylsilyl)amido] (**5**), and [bis-3,3′-(1,3-propanediyldiimino)-1-phenyl-2-butene-1-onato]erbium[bis(trimethylsilyl)amido] (**6**). To illustrate the effect of subtle alkyl substitutions on the ligand backbone further, the synthesis and characterization of [bis-5,5′-(2,2-dimethyl-1,3-propanediyldiimino)-2,2-dimethyl-4-hexene-3-onato]samarium[bis(trimethylsilyl)amido] (**4**) is included. In **4**, the central carbon (C(6)) of the propylene bridge supports

(6) (a) Schuetz, S. A.; Day, V. W.; Rheingold, A. L.; Belot, J. A. *J. Chem. Soc., Dalton Trans.* **2003**, *22*, 4303. (b) Yu, L.-B.; Yao, Y.-M.; Shen, Q.; Zhang, J.; Wu, L.-X.; Ye, L. *Chin. J. Chem.* **2003**, *21*, 442. (c) Schuetz, S. A.; Day, V. W.; Clark, J. L.; Belot, J. A. *Inorg. Chem. Commun.* **2002**, *5*, 706. (d) Evans, W. J.; Fujimoto, C. H.; Ziller, J. W. *Polyhedron* **2002**, *21*, 1683. (e) Schuetz, S. A.; Day, V. W.; Sommer, R. D.; Rheingold, A. L.; Belot, J. A. *Inorg. Chem.* **2001**, *40*, 5292. (f) Evans, W. J.; Fujimoto, C. H.; Ziller, J. W. *J. Chem. Soc., Chem. Commun.* **1999**, 311. (g) Liu, Q.; Ding, M.; Lin, Y.; Xing, Y. *Polyhedron* **1998**, *13*−*14*, 2327. (h) Liu, Q.; Ding, M. *J. Organomet. Chem.* **1998**, *553*, 179. (i) Liu, Q.; Ding, M.; Lin, Y.; Xing, Y. *Polyhedron*, **1998**, *17*, 555. (j) Dube, T.; Gambarotta, S.; Yap, G. *Organometallics* **1998**, *17*, 3967. (k) Liu, Q.; Ding, M.; Lin, Y.; Xing, Y. *J. Organomet. Chem.* **1997**, *548*, 139.
(7) Yamada, S. *Coord. Chem. Rev.* **1999**, *190*−*192*, 537.
(8) (a) Cai, Y. P.; Ma, H. Z.; Kang, B. S.; Su, C. Y.; Zhang, W.; Sun, J.; Xiong, Y. L. *J. Organomet. Chem.* **2001**, *628*, 99. (b) Blech, P.; Floriani, C.; Chiesivilla, A.; Guastini, C. *J. Chem. Soc., Dalton Trans.* **1990**, 3557.
(9) (a) Lin, M.-H.; RajanBabu, T. V. *Org. Lett.* **2002**, *4*, 1607. (b) Runte, O.; Priermeier, T.; Anwander, R. *J. Chem. Soc., Chem. Commun.* **1996**, 1385.

gem-dimethyls, which significantly changes the six-membered diamino chelate-ring geometry. Complexes **1** and **5** differ only in their rare-earth elements, whereas **6** has phenyl substituents replacing the bulky, frontal ^{t}Bu groups of **5**. This modification not only makes the rare-earth ion more accessible to substrate approach in both the derived amino and alkoxide complexes but also creates more freedom for axial-ligand motion. These syntheses explicitly demonstrate that this general ligand scaffold tolerates both various peripheral substituents and changing Ln^{3+} radii in affording discrete, mononuclear complexes. The isolated alkoxides also present mononuclear complexes when sterically demanding aryl alcohols occupy the apical coordination site; however, when the alcohol bulk is drastically reduced (i.e., EtOH) the formation of a highly symmetric, neutral trinuclear species is observed. All of these complexes are fully characterized using a variety of spectroscopic techniques including elemental analyses and single-crystal X-ray diffraction and are amenable to large-scale, reproducible preparations.

Experimental Section

Materials and Methods. All reactions were carried out under an atmosphere of dry dintrogen (passage over two 1.5-m glass columns containing Drierite and molecular sieves) using standard Schlenk and glovebox techniques. The synthesis of [tris(bis(trimethylsilyl)amido]lanthanides and bis-5,5′-(1,3-propanediyldiimino)-2,2-dimethyl-4-hexene-3-one were accomplished using literature preparations.[6e] 2,6-Di(*tert*-butyl)-4-methyl phenol (Aldrich) was doubly sublimed ($\sim 10^{-4}-10^{-5}$ Torr) before use and stored in the glovebox, whereas 1-phenyl-1,3-butanedione (Aldrich) was used as received. Heptane (C_7H_{16}, EM Science) and pentane (C_5H_{12}, Fisher) were dried and distilled from CaH_2. Toluene (C_7H_8) and ethanol (EtOH) were dried and distilled from sodium. ^{1}H and ^{13}C NMR were recorded on a Bruker DRX Avance 500-MHz spectrometer (^{1}H frequency) or a DRX Avance 400-MHz spectrometer (^{1}H frequency) using J. Young NMR tubes into which dry deuterated solvents were vacuum transferred from storage bulbs containing a Na/K alloy. Elemental analyses were performed by Midwest Microlabs (Indianapolis, IN), and the melting points (uncorrected) were collected on a modified Mel-Temp II apparatus providing digital thermocouple readouts.

Synthesis of Bis-3,3′-(1,3-propanediyldiimino)-1-phenyl-2-butene-1-one (3).[10] In a 500-mL round-bottom flask, 20 g (0.12 mol) of 1-phenyl-1,3-butanedione was dissolved in 300 mL of EtOH. An addition funnel was charged with 4.6 g (0.062 mol) of 1,3-diaminopropane in 75 mL of EtOH, and this solution was added dropwise (2 drops/s) to completion. The reaction was heated to reflux overnight, and then cooled and poured into 250 mL of H_2O, affording a white precipitate. This precipitate was isolated by simple vacuum filtration on a glass frit funnel (M porosity) and recrystallized from 200 mL of dry, boiling C_7H_{16} as colorless needles. The collected crystals were then dissolved in 200 mL of C_6H_6 and further dried by continuous azeotropic distillation until a constant boiling point was observed. The resulting ligand was again dried in vacuo ($10^{-4}-10^{-5}$ Torr at 40 °C) for 24 h. Yield: 41% (9.2 g); mp: 97−100 °C; ^{1}H NMR (δ, $CDCl_3$): 2.03 (m, 2H), 2.09 (s, 6H), 3.50 (m, 2H), 5.71 (s, 2H), 7.39 (b, 1H), 7.40 (b, 1H), 7.41 (b, 1H), 7.41 (b, 1H), 7.42 (b, 1H), 7.84 (b, 1H), 7.85 (b, 1H), 7.86 (b, 1H), 7.86 (b, 1H), 7.87 (b, 1H), 11.54 (b, 2H); ^{13}C NMR (δ, $CDCl_3$): 19.6, 30.3, 40.2, 92.7, 127.1, 128.4, 130.5, 140.5, 165.2, 188.4; Anal. Calcd for $C_{23}H_{26}N_2O_2$: C, 76.21; H, 7.23; N, 7.73. Found: C, 76.59; H, 7.10; N, 7.78.

Synthesis of [Bis-5,5′-(2,2-dimethyl-1,3-propanediyldiimino)-2,2-dimethyl-4-hexene-3-onato]samarium[bis(trimethylsilyl)-amido] (4). A 14/20, 100-mL Schenk flask is charged with 0.823 g (1.30 mmol) of tris(bis(trimethylsilyl)amido)samarium (glovebox), sealed with a septum, interfaced to a Schlenk line, and charged with 40 mL of C_7H_{16}. In a separate 14/20, 100-mL round-bottom flask, 0.457 g (1.30 mmol) of bis-5,5′-(2,2-dimethyl-1,3-propanediyldiimino)-2,2-dimethyl-4-hexene-3-one is dissolved in 40 mL of C_7H_{16}. The ligand solution is then added to the samarium flask via syringe in one aliquot. Under flowing N_2, the septum is replaced with a reflux condenser, and the reaction is heated to reflux for 12 h. The homogeneous, dull-yellow mother liquor is then concentrated in vacuo (~10 mL) and cooled to −10 °C. Pale-yellow crystals are harvested after 4 days. Yield: 67.1% (0.561 g); mp: 152−154 °C; ^{1}H NMR (δ, C_6D_6): −4.14, −2.30, −2.02, −0.79, 0.08, 0.15, 0.60, 0.66, 0.76, 0.86, 1.05, 1.11, 1.27, 1.41, 1.55, 1.87, 2.12, 4.13, 4.59, 6.49, 6.88, 7.73, 10.61; ^{13}C NMR (δ, C_6D_6): 5.9, 18.9, 20.5, 28.1, 29.2, 29.6, 54.3, 99.9, 174.9, 195.9. Anal. Calcd for $C_{27}H_{54}N_3O_2Si_2Sm$: C, 49.19; H, 8.26. Found: C, 49.21; H, 8.15.

Synthesis of [Bis-5,5′-(1,3-propanediyldiimino)-2,2-dimethyl-4-hexene-3-onato]erbium[bis(trimethylsilyl)amido] (5). To a 250-mL Schlenk flask containing 1.81 g (2.79 mmol) of tris(bis-[trimethylsilyl]amido)erbium dissolved in 100 mL of C_7H_{16}, we added 0.900 g (2.79 mmol) of bis-5,5′-(1,3-propanediyldiimino)-2,2-dimethyl-4-hexene-3-one into 50 mL of C_7H_{16} via a syringe. The solution was stirred and heated to reflux overnight, the organics were removed in vacuo, and the crude product was recrystallized (24 h) from 10 mL of C_5H_{12} at −10 °C as pale-pink crystals. Yield: 82% (1.48 g); mp: 153.8−154.9 °C; ^{1}H NMR (δ, C_6D_6): 0.05 (s, 18H), 1.00 (m, 2H), 1.34 (b, 6H), 4.90 (m, 4H), 6.74 (b, 2H), 10.62 (b, 2H); ^{13}C NMR (δ, C_6D_6): 2.6, 6.1, 19.2, 20.8, 29.4, 29.8, 37.2, 54.6, 100.1, 175.2, 196.2; Anal. Calcd for $C_{25}H_{50}N_3O_2Si_2Er$: C, 46.33; H, 7.78. Found C, 46.55; H, 7.61.

Synthesis of [Bis-3,3′-(1,3-propanediyldiimino)-1-phenyl-2-butene-1-onato]erbium[bis(trimethylsilyl)amido] (6). In a 100-mL Schlenk flask, 1.119 g (1.726 mmol) of tris[bis(trimethylsilyl)-amido]erbium was dissolved in 30 mL of C_7H_8. To this solution, we added 0.6256 g (1.726 mmol) of **3** dissolved in warm C_7H_8. The reaction was heated to reflux overnight, cooled to room temperature, and concentrated in vacuo, and the title compound was recrystallized from the mother liquor after 12 h at −18 °C as pink crystals. Yield: 60.3% (0.7043 g); mp: 140−142 °C (dec); ^{1}H NMR (δ, C_6D_6): −42.16, −28.59, 0.01, 2.09, 4.53, 7.02, 10.28, 13.73, 27.93; ^{13}C NMR (δ, C_6D_6): −63.61, −43.22, −32.63, 2.34, 5.80, 21.29, 22.00, 79.46, 106.65, 125.71, 135.58; Anal. Calcd for $C_{29}H_{42}N_3O_2Si_2Er \cdot {}^1/_2C_7H_8$: C, 53.17; H, 6.32. Found C, 53.11; H, 6.22 (the presence of toluene was confirmed by X-ray diffraction).

Representative Aryloxide Synthesis of [Bis-5,5′-(1,3-propanediyldiimino)-2,2-dimethyl-4-hexene-3-onato]lanthanide[2,6-bis(*tert*-butyl)-4-methylphenoxide]. In a 100-mL Schlenk flask 0.47 mmol [bis-5,5′-(1,3-propanediyldiimino)-2,2-dimethyl-4-hexene-3-onato]lanthanide[bis(trimethylsilyl)amido] was dissolved in 40 mL of C_5H_{12}, and 0.11 g (0.47 mmol) of 2,6-di(*tert*-butyl)-4-methyl phenol in 40 mL of C_5H_{12} was added via a syringe. The solution was stirred and heated to reflux overnight, the organics were removed in vacuo, and the crude products were recrystallized (24 h) from ~5 mL of C_7H_8 at −18 °C.

[Bis-5,5′-(1,3-propanediyldiimino)-2,2-dimethyl-4-hexene-3-onato]erbium[2,6-bis(*tert*-butyl)-4-methylphenoxide] (7 and Solvent Polymorph 9). Yield: 82% (0.28 g, pale pink); mp: 158.0−

Table 1. Crystallographic Data for Compounds **4**−**11**[a]

	4	**5**	**6**	**7**
formula	$C_{27}H_{54}N_3O_2Si_2Sm$	$C_{25}H_{50}N_3O_2Si_2Er$	$C_{32.50}H_{46}N_3O_2Si_2Er$	$C_{41}H_{63}N_2O_3Er$
fw	659.26	648.12	734.16	799.19
cryst syst, space group[b]	monoclinic, $P2_1/c$ (No. 14)	monoclinic, $P2_1/c$ (No. 14)	triclinic, $P\bar{1}$ (No. 2)	monoclinic, $P2_1/n$ (No. 14[f])
a (Å)	12.319(3)	10.563(1)	14.245(1)	11.831(2)
b (Å)	16.058(4)	25.738(1)	15.547(1)	21.780(4)
c (Å)	17.752(4)	12.000(1)	17.105(1)	15.584(3)
α (deg)	90.000	90.000	105.201(1)	90.000
β (deg)	109.132(3)	107.127(1)	102.598(1)	92.397(4)
γ (deg)	90.000	90.000	100.237(1)	90.000
V (Å^3)	3317.8(13)	3117.7(3)	3454.7(3)	4012.2(13)
Z, ρ_{calcd} (Mg/m^3)	4, 1.320	4, 1.381	4, 1.412	4, 1.323
μ (Mo Kα) (mm^{-1})	1.867	2.792	2.529	2.128
cryst size (mm^3)	0.21 × 0.10 × 0.09	0.21 × 0.20 × 0.12	0.10 × 0.09 × 0.08	0.10 × 0.08 × 0.06
data completeness (max $\theta_{Mo\,K\alpha}$)	95.8% (28.32)	99.8% (28.35)	99.7% (28.30)	99.8% (28.33)
absorption correction	empirical	empirical	empirical	empirical
min/max transmission	0.604/0.415	0.896/1.000	0.914/1.000	0.775/1.000
largest diff. peak/hole (e$^-$/A^3)	2.068/−1.060	0.831/−0.566	1.223/−0.809	2.399/−1.549
temp (K)	100(2)	173(2)	173(2)	173(2)
no. of reflns (collected/unique)	38 927/7898	33 544/7757	50 028/17 139	46 618/9990
R_1[c] ($I > 2\sigma I$)	0.034(6555)	0.024(6535)	0.0321 (12571)	0.052(7729)
wR_2[d] (unique reflns)	0.076(7898)	0.048(7757)	0.0564(17 139)	0.100(9990)
GOF indicator[e]	0.997	0.948	0.830	0.990

	8	**9**	**10**	**11**
formula	$C_{41}H_{63}N_2O_3Sm$	$C_{41}H_{63}N_2O_3Er$	$C_{48.50}H_{59}N_2O_3Er$	$C_{92}H_{101}N_6O_8Er_3$
fw	782.28	753.13	885.24	1920.57
cryst syst, space group[b]	monoclinic, $P2_1/n$ (No. 14[f])	monoclinic, $P2_1/n$ (No. 14[f])	triclinic, $P\bar{1}$ (No. 2)	monoclinic, $P2(1)/c$ (No. 14)
a (Å)	11.715(2)	13.600(1)	13.602(1)	21.573(2)
b (Å)	22.216(3)	20.226(1)	13.700(1)	16.529(2)
c (Å)	15.548(2)	14.231(1)	13.708(1)	23.422(3)
α (deg)	90.000	90.000	78.515(5)	90.000
β (deg)	92.469(2)	106.035(1)	60.973(3)	93.678(2)
γ (deg)	90.000	90.000	78.482(3)	90.000
V (Å^3)	4042.9(9)	3762.1(3)	2173.0(2)	8334.7(16)
Z, ρ_{calcd} (Mg/m^3)	4, 1.285	4, 1.330	2, 1.353	4, 1.531
μ (Mo Kα) (mm^{-1})	1.489	2.265	1.972	3.052
cryst size (mm^3)	0.30 × 0.20 × 0.20	0.16 × 0.10 × 0.09	0.10 × 0.07 × 0.05	0.50 × 0.32 × 0.32
data completeness (max $\theta_{Mo\,K\alpha}$)	93.6% (28.30)	99.9% (28.30)	99.3% (28.31)	99.9% (28.34)
absorption correction	SADABS	empirical	empirical	empirical
min/max transmission	0.759/1.000	0.850/1.000	0.922/1.000	0.704/1.000
largest diff peak/hole (e$^-$/A^3)	1.095/−0.841	1.054/−0.331	1.837/−0.654	1.797/−0.642
temp (K)	150(2)	173(2)	173(2)	173(2)
no. of reflns (collected/unique)	25 140/9400	40 286/9322	25 221/10 729	115 421/20 772
R_1[c] ($I > 2\sigma I$)	0.042(7206)	0.0253(7395)	0.051(8441)	0.032(17 135)
wR_2[d] (unique reflections)	0.095(9400)	0.054(9322)	0.110(10 729)	0.091(20 772)
GOF indicator[e]	1.036	0.891	0.977	1.062

[a] G. M. Sheldrick, *SHELXTL*, version 5.1; Bruker-AXS: Madison, WI, 1999. [b] Henry, N. F. M.; Lonsdale, K., Eds. *International Tables for X-ray Crystallography*, Vol. 1: Symmetry Groups; Kyntoch Press, U.K., 1969. [c] $R_1 = \sum | |F_o| - |F_c| | / \sum |F_o|$. [d] $R_2 = [(\sum w(|F_o| - |F_c|)^2 / \sum w(|F_o|^2)^2)]^{1/2}$. [e] GOF: $[(\sum w(|F_o| - |F_c|)^2 / (N_{obs} - N_{param})]^{1/2}$. [f] $P2_1/n$ is an alternate setting for $P2_1/c - C2_h^5$ (No. 14).

160.5 °C (dec); ^{1}H NMR (δ, C_6D_6): −53.28 (b, H), −13.46 (b, H), −6.20 (b, H), −2.43 (b, H), 1.39 (s, H), 2.22 (s, H), 2.29 (b, H), 4.77 (b, H), 7.12 (s, H), 7.20 (s, H), 8.86 (b, H); ^{13}C NMR (δ, C_6D_6): −55.7, −42.9, −21.1, −16.8, 13.4, 21.4, 29.9, 30.3, 40.7, 73.4, 95.6, 101.0, 125.7, 129.3, 137.9; Anal. Calcd for $C_{34}H_{55}N_2O_3Er \cdot {}^1/_3C_7H_8$: C, 59.15; H, 7.88. Found C: 59.30; H, 7.82 (the presence of toluene was confirmed by X-ray diffraction).

[Bis-5,5′-(1,3-propanediyldiimino)-2,2-dimethyl-4-hexene-3-onato]samarium[2,6-bis(*tert*-butyl)-4-methylphenoxide] (8). Yield: 81% (0.26 g, pale yellow); mp: 153.5−155.0 °C (dec); ^{1}H NMR (δ, C_6D_6) −23.84 (b, H), −6.56 (b, H), −3.68 (b, H), −2.79 (b, H), 0.84 (s, 2H), 0.99 (s, H), 1.38 (b, 2H), 2.09 (s, H), 2.22 (b, 2H), 2.73 (s, 3H), 3.52 (b, H), 4.78 (b, 2H), 7.05 (b, H), 8.02 (b, H), 8.51 (b, H); ^{13}C NMR (δ, C_6D_6) 20.35. 22.39, 28.89, 33.78, 36.76, 38.04, 43.40, 101.43, 124.91, 126.71, 139.18, 163.54, 178.82, 197.44; Anal. Calcd for $C_{34}H_{55}N_2O_3Sm$: C, 59.17; H, 8.03. Found C, 59.29; H, 7.98.

[Bis-3,3′-(1,3-propanediyldiimino)-1-phenyl-2-butene-1-onato]-erbium[2,6-bis(*tert*-butyl)-4-methylphenoxide] (10). Yield: 71% (0.23 g, pale pink); mp: 161.0−163.0 °C (dec); ^{1}H NMR (δ, C_6D_6): −49.82 (b), −14.51 (b), −6.99 (b), −5.70 (b), 1.18 (b), 2.02 (b), 2.16 (b), 4.44 (b), 6.90 (b), 11.91 (b), 16.70 (b), 37.57 (b); ^{13}C NMR (δ, C_6D_6): 137.13, 135.77, 131.41, 125.64, 98.51, 92.56, 67.37, 66.64, 34.06, 30.22, 28.44, 21.28, 12.313, −17.58, −46.19, −60.44, −145.52; Anal. Calcd for $ErN_2C_{38}H_{47}O_3$: C, 61.09; H, 6.34. Found: C, 60.69; H, 6.37.

Synthesis of the Er-Oxo-Alkoxy Cluster (11). In a 100-mL Schlenk flask, 1.0 g (1.4 mmol) of **7** was dissolved in 30 mL of C_7H_8. To this solution, we added 0.065 g (1.4 mmol, 0.083 mL) of dried EtOH dissolved in 30 mL of C_7H_8. This solution was then

Table 2. Average Metal−Ligand Bond Lengths (Å) in the Coordination Polyhedra of **4**−**10**

		Schiff base			axial ligand	
compd	type	length	type	length	type	length
4	Sm−O	2.218(2,9,9,2)	Sm−N	2.466(2,6,6,2)	Sm−N	2.307(2)
8	Sm−O	2.206(2,0,0,2)	Sm−N	2.464(3,3,3,2)	Sm−O	2.143(2)
average	Sm−O	2.212(2,14,7,4)	Sm−N	2.465(3,7,5,4)		
5	Er−O	2.138(2,3,3,2)	Er−N	2.371(2,2,2,2)	Er−N	2.230(2)
6	Er−O	2.143(2,13,7,4)	Er−N	2.371(3,10,6,4)	Er−N	2.226(3,1,1,2)
7	Er−O	2.140(3,8,8,2)	Er−N	2.369(4,6,6,2)	Er−O	2.073(3)
9	Er−O	2.131(2,1,1,2)	Er−N	2.366(2,8,8,2)	Er−O	2.081(2)
10	Er−O	2.144(3,18,18,2)	Er−N	2.366(3,13,13,2)	Er−O	2.071(3)
average	Er−O	2.140(2,21,9,12)	Er−N	2.369(3,16,7,12)	Er−O	

stirred overnight and concentrated in vacuo, and pale-pink crystals formed after 7 days at −18 °C. ^{1}H NMR (δ, C_6D_6): −28.08 (b), 0.049 (s), 0.95 (b), 1.24 (b,d), 2.07 (s), 5.08 (b), 6.98 (s), 7.05 (s), 7.30 (b), 10.17 (b), 13.56 (b), 27.49 (s); Anal. Calcd for $C_{71}H_{77}N_6O_8Er_3 \cdot C_7H_8$: C, 53.96; H, 4.93. Found: C, 53.06; H, 5.99.

General Homopolymerizations of *rac*-Lactide and ϵ-Caprolactone. In a 100-mL Schlenk flask either 1.44 g of *rac*-lactide or 1.14 g of ϵ-caprolactone (10.0 mmol) was dissolved in 65 mL of C_7H_8 (0.154 M). While stirring, 2.00 mL of a 0.0500 M toluene catalyst solution (6.0 mL of a 0.0167M solution for ϵ-caprolactone polymerization) was added in one portion, and the reaction was stirred at either 26 or 70 °C for 30 min. The polymerization reaction was subsequently quenched with 20 mL of ^{i}PrOH, and the polymer was precipitated with excess pentane (∼150 mL). The resulting colorless solid was dried in vacuo (26 °C at $\sim 10^{-4}-10^{-5}$ Torr) to a constant weight.

X-ray Structure Determinations. Lattice constants, space groups, final agreement factors, and other relevant crystallographic data for **4**−**11** are given in Table 1. Complete hemispheres of diffraction data were collected for each compound with a Bruker SMART APEX CCD area detector using 0.30°-wide ω scans and graphite-monochromated Mo Kα radiation. X-rays for each study were provided by a fine-focus-sealed X-ray tube operated at 50 kV and 40 mA. Frame data (10 s, 0.30°-wide ω scans) were collected using the Bruker SMART software package, and final lattice constants were determined with the Bruker SAINT software package. The Bruker SHELXTL-NT software package was used to solve and refine each structure. "Direct methods" was used to solve each structure, and the resulting parameters were refined with F^2 data to convergence using counterweighted full-matrix least-squares techniques and a structural model that incorporated anisotropic thermal parameters for all ordered nonhydrogen atoms, including most of the solvent nonhydrogen atoms. Isotropic thermal parameters were incorporated for all hydrogen atoms and several carbon atoms of disordered toluene solvent molecules of crystallization. The highest peaks (2.40−0.83 e$^-$/Å^3) in the final difference Fouriers for **4**−**11** were within 1.07 Å of a metal atom or a carbon atom of a disordered toluene molecule of crystallization. Discussions outlining the treatment of hydrogen atoms and solvent disorder in structures **4**−**11** are given in Supporting Information.

Crystals of **4**−**11** have several noteworthy features. Crystals of **4** and **5** are isomorphous with previously reported Er^{3+} and Sm^{3+} complexes[6c,e] and although the lattice constants and space groups for **7** and **8** would tend to indicate another isomorphous pair, this is not the case. If crystals of **7** and **8** contained the same metal, then they would be rigorous polymorphs. The asymmetric units of **7** and **9** contain different numbers of toluene solvent molecules of crystallization; these two crystalline forms of solvated $[O_2N_2C_{19}H_{32}]Er[OC_6H_2CH_3(t\text{-}C_4H_9)_2]$ are therefore solvate pseudopolymorphs. The two crystallographically independent $[O_2N_2C_{23}H_{24}]Er[N(Si(t\text{-}C_4H_9)_3)_2]$ molecules in the asymmetric unit of **6** are related by a noncrystallographic inversion center near ($^1/_4$, 0, $^1/_4$) in the unit cell, and the center of the ring for the toluene solvent molecule of crystallization is located near ($^3/_4$, $^1/_2$, $^1/_4$) in the unit cell. Atoms in the asymmetric unit of **6** are labeled to reflect this pseudosymmetry. Average bond lengths in the coordination spheres of **4**−**10** are given with estimated standard deviations in Table 2. Structurally significant parameters derived from the final atomic coordinates of **4**−**10** are presented in Table 3.

Table 3. Structurally Significant Parameters Derived from Final Atomic Coordinates of **4**−**10**[16]

compd	fold 1[a]	fold 2[b]	ax	τ	ΔL	ΔM	ΔMe
4	28.3, 29.6	4.0, 7.4	4.1	0.08	0.05	0.83	2.84, 2.82
5	25.7, 44.1	8.7, 16.3	1.6	0.36	0.19	0.89	2.82, 2.73
6 molecule 1	32.1, 44.8	3.2, 15.8	3.7	0.32	0.17	0.92	2.87, 2.80
6 molecule 2	33.2, 38.4	2.2, 9.3	2.0	0.17	0.09	0.89	2.76, 2.82
7	38.1, 36.2	9.8, 9.2	7.6	0.02	0.01	0.86	3.15, 3.53
							3.38, 3.51
8	38.7, 39.6	11.0, 10.4	4.0	0.10	0.06	0.93	3.38, 3.57
							3.41, 3.77
9	36.5, 33.0	10.6, 5.5	3.9	0.14	0.07	0.82	3.36, 3.42
							3.35, 3.35
10	25.7, 21.6	2.5, 6.9	1.6	0.04	0.14	0.80	3.26, 3.23
							3.26, 3.63

[a] Defined as the dihedral angle between the square base and seven-atom ketoiminate half. [b] Defined as the fold of the KI chelate ring about the Ln^{3+} ON vector.

Results and Discussion

The three acyclic ketoiminates used to ligate the anhydrous, solvent-free rare earth ions, bis-3,3′-(1,3-propanediyldiimino)-1-phenyl-2-butene-1-one (**3**), bis-5,5′-(1,3-propanediyldiimino)-2,2-dimethyl-4-hexene-3-one, and bis-5,5′-(2,2-dimethyl-1,3-propanediyldiimino)-2,2-dimethyl-4-hexene-3-one[6c] were synthesized by reacting the appropriate diketone with 1,3-propanediamine.[7,10] The diketone for **3** is commercially available, but the starting material for the two others must be isolated from the NaH-initiated Claisen condensation of pinacolone with ethyl acetate.[11] Although the chelators are inexpensively and straightforwardly synthesized and isolated in high yields and analytical purity (note: rigorous removal of adventitious H_2O and EtOH must be undertaken via azeotropes), which adds to their desirability, these frameworks were not designed for convenience but rather to accommodate large f elements exhibiting low

(10) (a) McCarthy, P. J.; Martell, A. E. *Inorg. Chem.* **1967**, *6*, 781. (b) McCarthy, P. J.; Hovey, R. J.; Ueno, K.; Martell, A. E. *J. Am. Chem. Soc.* **1955**, *77*, 5820. (c) Although this ligand is known, we report its synthesis and characterization as the necessary H_2O- and EtOH-free compound.

(11) Adams, J. T.; Hauser, C. R. *J. Am. Chem. Soc.* **1944**, *66*, 1220.

Scheme 1. Alcoholysis Reaction Pathways and Products Involving Mononuclear Amino Complexes **1**, **5**, and **6**[a]

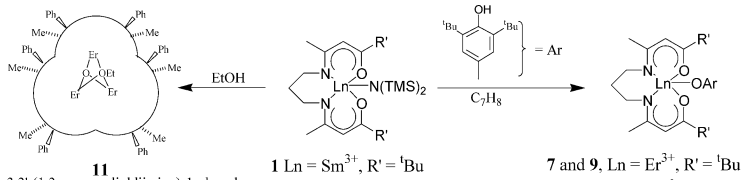

11
(Bis-3,3'-(1,3-propanediyldiimino)-1-phenyl-2-buten-1-one)erbium(μ_3-O)(μ_3-OEt) trimer [$Er_3C_{71}N_6O_8H_{77}$]

1 Ln = Sm^{3+}, R' = ^{t}Bu
5 Ln = Er^{3+}, R' = ^{t}Bu
6 Ln = Er^{3+}, R' = Ph

7 and **9**, Ln = Er^{3+}, R' = ^{t}Bu
8 Ln = Sm^{3+}, R' = ^{t}Bu
10 Ln = Er^{3+}, R' = Ph

[a] The $HN(TMS)_2$ byproduct has been omitted.

coordination numbers. Specifically, on the basis of failed attempts to isolate similar lanthanide complexes with a smaller ethylene spacer bisected by the idealized mirror plane, we rationalized that the slightly larger propyl unit would increase the requisite N···N separation for larger lanthanide-metal capture.[6e] Second, the avoidance of aromatic groups within the ketoiminate backbone would preclude potential intermolecular π-stacking interactions, which have been implicated in the formation of anhydrous, dinuclear Ln_2L_3 (L = Schiff base)[8a] that are incapable of optimally serving as single-site catalysts.

Ligand metalation is accomplished by reacting the protio ketoiminate with $Ln[N(TMS)_2]_3$ in refluxing C_7H_{16}, the silylamide route.[12a,b] The homoleptic amido starting materials were prepared from dried $Ln(OTf)_3$ using our previously reported procedure.[6e] The use of "innocent" linear hydrocarbons during metalation avoids metal ion solvation, whereas the silylamide-mediated lanthanide insertion mutes the potential formation of "ate" complexes or μ-bridging[8b] halides from $LnCl_3$ preparations.[8b] The as-isolated monoamidos are themselves active catalysts whose metal coordination spheres are not crowded by spurious ligands, the $HN(TMS)_2$ byproduct is easily removed from stoichiometric reactions, and the monodentate ligand can be rapidly replaced using acid−base chemistry without degradation of the Schiff-base scaffold (vide infra). Although RajanBabu,[9a] Anwander,[9b] and Evans[6d] have successfully employed both silylamide and chloride routes for mononuclear and dinuclear yttrium salen complexes that are catalytically active,[9b] the metal ion in these examples is further stabilized through coordination to a Lewis base (i.e., THF) from either adventitious solvent or starting material solvates. This seemingly subtle solvate increase in coordination number can drastically diminish the catalytic activity.[13a,b]

To determine ketoiminato stability toward amido substitution and develop general routines to produce more nucleophilic monoanions (i.e., alkoxides), we accomplished direct conversion of the mononuclear amidos to mononuclear alkoxides by the stoichiometric reaction of **1**, **5**, and **6** with sterically demanding 2,6-di(*tert*-butyl)-4-methyl phenol (BHT) in C_5H_{12}[2a] (Scheme 1). The crude alkoxide complexes are readily purified as innocent solvates by recrystallization to give X-ray-quality crystals in excellent yield and analytical purity. Although the ketoiminate framework does not degrade in the presence of acidic phenols, ethanol, or free $HN(TMS)_2$, compounds **7** and **8** are completely *inactive* for the solution polymerization of propylene oxide, ϵ-caprolactone, butyrolactone, and *rac*-lactide. These results parallel those of Hubert-Pfalzgraf, who also observed no polymerization activity of polar monomers with trivalent rare earths coordinated to bulky aryloxide monoanions.[14] This is attributed to substrate inaccessibility at the metal center and is further supported by noting that the less sterically demanding complex, **10**, acts as an active polymerization catalyst for these monomers. Analogously, we sought to assess requisite alkoxide sterics for isolating discrete mononuclear complexes by employing ethanol as the Brønsted acid (Scheme 1). This extreme reduction in alcohol bulk afforded a neutral, trimeric, oxo−alkoxide Er^{3+} cluster (**11**). Although the origin of the bridging μ_3-oxo dianion remains speculative, adventitious H_2O or oxo-atom abstraction are the most likely sources.[15]

The solid-state structure of **4** exhibits a mononuclear, five-coordinate Sm^{3+} ion in a slightly distorted (τ = 0.08)[16] square-pyramidal environment. The average Sm−O and Sm−N ketoiminato bond lengths[17] are 2.218 (2,9,9,2) and 2.466 (2,6,6,2) Å, respectively, and the apical 2.307(2)-Å Sm−N(3) amido bond distance 4.1° from the ketoiminato N_2O_2 square base normal. The Sm^{3+} ion is displaced 0.83 Å from the ±0.05-Å S_4-ruffled N(1), N(2), O(1), O(2) mean plane. The canting of the apical amido and the Schiff-base S_4 ruffling impose chirality upon the metal center, and both enantiomers are present within the crystal. The six-membered diamino chelate ring, bearing the *gem*-dialkyl substituent at C(6), adopts the chair conformation previously reported[6c] for the isomorphous erbium complex. This is in contrast to the unsubstituted six-membered diamine chelate rings in complexes **5**−**10**, all of which adopt the boat conformation without crystallographic disorder at the C(6) methylene carbon.[18]

(12) (a) Anwander, R. *Top. Curr. Chem.* **1996**, *179*, 33. (b) Anwander, R.; Runte, O.; Eppinger, J.; Gerstberger, G.; Herdtweck, E.; Spiegler, M. *J. Chem. Soc., Dalton Trans.* **1998**, 847.

(13) (a) Hessen, B. Presented at the 225th National Meeting of the American Chemical Society, New Orleans, LA, March 2003; paper INOR-919. (b) Gagne, M. R.; Stern, C. L.; Marks, T. J. *J. Am. Chem. Soc.* **1992**, *114*, 275.

(14) Daniele, S.; Hubert-Pfalzgraf, L. G.; Vaissermann, J. *Polyhedron* **2003**, *22*, 127.

(15) Caulton, K. G.; Hubert-Pfalzgraf, L. G. *Chem. Rev.* **1990**, *90*, 969.

(16) For the τ calculation and its significance in five-coordinate square-planar complexes, see: Addison, A. W.; Rao, T. N.; Reedijk, J.; van Rijn, J.; Verschoor, G. C. *J. Chem. Soc., Dalton Trans.* **1984**, 1349.

(17) Throughout this manuscript, a standard formalism of crystallography-derived estimated standard deviations is used to provide a more concise, yet comprehensive, synopsis of metrical parameters. Hence, the first number in parentheses following an average value of a bond length is the rms estimated standard deviation of an individual datum. The second and third numbers are the average and maximum deviations from the average value, respectively. The fourth number represents the number of individual measurements included in the average values.

The mononuclear complexes with the unsubstituted propyl bridge (**5**−**10**) have several common solid-state features. The polyhedron in each, defined by the coordinated oxygen and nitrogen atoms, is a distorted square pyramid, and the ketoiminato donor atoms define an S_4-ruffled square base. The extent of S_4 ruffling (ΔL in Table 3) ranges from 0.009 Å in **7** to 0.19 Å in **5**. Each Ln^{3+} ion is displaced (ΔM in Table 3) by 0.83−0.93 Å from this square base. The average ketoiminato Er−O bond lengths range from 2.131 (2,1,1,2) Å in **9** to 2.144 (3,18,18,2) Å in **10** and average 2.140 (2,21,9,12) Å for all six mononuclear propyl-bridged erbium-containing molecules reported herein. The corresponding ketoiminato Er−N bond lengths range from 2.365 (2,8,8,2) Å in **9** to 2.371 (2,2,2,2) Å in **5** and average 2.369 (3,16,7,12) Å for all six mononuclear erbium complexes. The corresponding ketoiminato Sm−O and Sm−N bond lengths of 2.206 (2,0,0,2) and 2.464(3,3,3,2) Å in **8** are completely consistent with the 0.07-Å larger ionic radius of Sm^{3+} relative to Er^{3+}. The axial Er−N(3) bonds range from 2.225 (2) Å in **6** to 2.230 (2) Å in **5**. The axial Er−O(3) bonds range from 2.071 (3) Å in **10** to 2.081 (2) Å in **9**. The unsubstituted propyl bridge in each of these complexes is part of a six-membered ($-Ln-N_1-C_5-C_6-C_7-N_2-$) diamino chelate ring that adopts an energetically unfavorable boat conformation. This chelate ring conformation produces a relatively short 2.6−2.7-Å Ln···H contact within each complex to a diastereotopic hydrogen on C(6) and may represent a stabilizing agostic interaction. It is particularly noteworthy that this supposition is supported by a decrease of the ^{13}C $J_{C(6)-H}$ values when compared with the free ligand.[19]

The axial Ln−O(3) and Ln−N(3) bonds in all of the mononuclear species make angles between 1.6−7.6° with the normals to their square-base mean planes. This canting ($\angle$ax in Table 3) is the cumulative result of sterically induced distortions of the prochiral complex from idealized C_s symmetry and, in conjunction with the S_4 ruffling, produces a form of "conformational racemic chirality".[20]

The solid-state structures of the six amido and aryloxide complexes, **5**−**10**, share many structural similarities, and their salient metrical parameters are summarized in Table 2. Although none of these molecules possess rigorous crystallographic symmetry, each approximates prochiral C_s-*m* to a varying degree. The idealized mirror plane would always contain the lanthanide ion, the axially coordinated nitrogen or oxygen atom (N(3) and O(3), respectively), and the C(6) central carbon atom of the propyl bridge as well as any substituents decorating this position. However, any structural distortion that removes this symmetry element introduces chirality at the metal center. Although this symmetry reduction could occur in many ways, five appear to be important in **5**−**10** because of geometric constraints inherent to the ligand sets, these include: (1) rotation of the amido or aryloxide ligands about the apical Ln−N or Ln−O bond, respectively; (2) rotations of either the TMS group about the N−Si bonds or the ^{t}Bu groups about the α-^{Ar}C−^{t}Bu bonds; (3) tilting of the axial Ln−N(3) or Ln−O(3) bonds relative to the square-base normal. (4) dissimilar folding of the two Schiff-base halves along the O···N polyhedral edges of this base; (5) rotation of the "frontal" Schiff base ^{t}Bu or Ph substituents about their ^{KI}C−^{t}Bu or ^{KI}C−Ph bonds. Because each mononuclear, chiral complex utilizes a centrosymmetric space group, both enantiomers are present in equal amounts within any crystal. Furthermore, crystalline **6** contains two separate enantiomeric pairs. The superposition of any enantiomeric pair would, therefore, show the extremes of a given symmetry-breaking distortion upon the prochiral species.

The structural constraints of the individual ligands in a given complex determine the nature and extent of any distortion from ideal C_s-*m* symmetry. Each Schiff-base ligand contains two planar ketoiminato halves (both containing one oxygen, one nitrogen, and six carbons) joined at a common point, the central carbon, C(6), of the propyl bridge. These planar halves can fold at the O···N square polyhedral edge and/or rotate about the vector through C(3) or C(9) and the midpoint of the corresponding O···N edge. S_4 ruffling of the square-base donor atoms is the structural manifestation of either planar ketoiminato half rotating relative to the other. The extent of Schiff base folding and/or rotation is restricted by the stereochemical requirements of the central methylene, C(6), whose six-membered diamine chelate ring always adopts the thermodynamically unfavorable boat conformation. The observance of diastereotopic Ln···H close contacts (without disorder at C(6)) and a decrease in the ^{13}C $J_{C(6)-H}$ coupling constant compared to that in the free ligand suggests an agostic interaction that conformationally "locks" this stereochemical pivot point. This structural feature is not observed in **2**, **4**, or the related propyl-bridged, mononuclear RAl^{3+}(Salpen) complexes of Atwood[21] and Nomura.[20]

The mononuclear structures observed for **7**−**10** bearing bulky apical aryloxides minimize nonbonded repulsions between the ^{t}Bu methyl groups, the apical oxygen, and the adjacent meta ring hydrogens in the free ligand. This C_{2v} structure places two methyl groups from each ^{t}Bu substituent close to the oxygen atom, O(3), and the third methyl close to the meta ring hydrogens. Similar alkyl group conformational orientation has been observed in homo- and heteroleptic lanthanide 2,6-di(^{t}Bu) phenoxide complexes.[22,23] Steric interactions between two of the methyl groups (C(28) and C(33)) and the first and third methylene carbon atoms (C(5) and C(7)) of the propyl bridge also force the aryloxide to

(18) Propyl-bridged Cu^{2+} Salen complexes have recently been found to contain this folded geometry; however, the central methylene is disordered over two positions with respect to the N_2O_2 plane, which is not the case in our systems; see Nathan, L. C.; Koehne, J. E.; Gilmore, J. M.; Hannibal, K. A.; Dewhirst, W. E.; Mai, T. D. *Polyhedron* **2003**, *22*, 887.

(19) For the use of $^1J_{C-H}$ coupling constants as indicators for Ln^{3+}···H−C interactions; see Gordon, J. C.; Giesbrecht, G. R.; Brady, J. T.; Clark, D. L.; Keogh, D. W.; Scott, B. L.; Watkin, J. G. *Organometallics* **2002**, *21*, 127.

(20) Nomura, N.; Ishii, R.; Akakura, M.; Aoi, K. *J. Am. Chem. Soc.* **2002**, *124*, 5938. A particularly important consequence within this paper is the possibility of "conformational racemic chirality" about the C_3H_6 bridge of an achiral aluminum Salen, thereby facilitating the site-controlled mechanism of isotactic polylactide formation.

(21) Atwood, D. A.; Harvey, M. J. *Chem. Rev.* **2001**, *101*, 37. (b) Atwood, D. A.; Hill, M. S.; Jegier, J. A.; Rutherford, D. *Organometallics* **1997**, *16*, 2659.

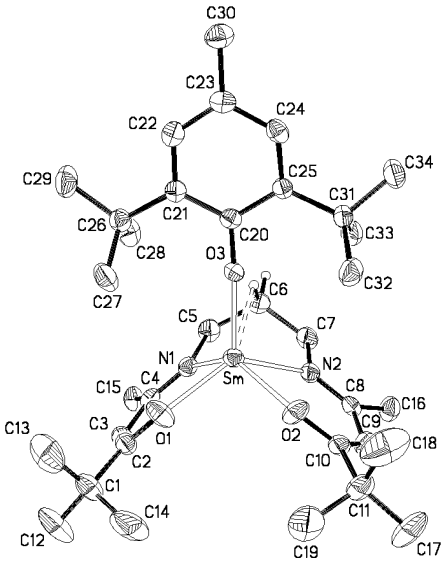

Figure 2. Molecular structure of mononuclear (KI)Sm^{3+} aryloxide (**8**) that is isomorphous with **7**.

adopt the general orientations shown in Figure 2 and restrict rotation about the Ln−O(3) bond. Thus, four methyl groups (C(27), C(28), C(32), and C(33)) impinge downward upon the ketoiminato C═O and C−N bonds and afford reasonably symmetrical Schiff-base folding along the O···N polyhedral edges. This bilateral steric effect is manifested in both decreased S_4 ruffling in the KI donor atoms and smaller τ values when compared to the parent aminos (Table 3). Unfortunately, these four methyl groups render the metal ion inaccessible to the incoming substrate and contribute to the complete solution-based polymerization inactivity toward strained (i.e., epoxides) and unstrained (i.e., lactones and lactides) polar monomers. Although much of the (BHT)Ln(KI) is sterically locked into a specific conformation, the Ln−O(3) bond cants off the square-base normal in the plane of its phenyl ring; the frontal ketoiminato substituents accommodate this motion by adopting different relative orientations. This is evident from the front (Figure 3A) and side (Figure 3B) views of the superimposed enantiomers of **7**. The metal and Schiff-base nonhydrogen atoms (excluding methyl carbons) for the racemic pair were superimposed by least-squares fitting to give a weighted rms deviation of 0.03 Å and an O(3)−Er−(O3′) angle of 14.1°.

The apical metal aryloxide bonds in **7**−**10** are significantly (∼0.06 Å) shorter than the ketoiminato Ln^{3+}−O bonds, as expected on the basis of charge density. The three independent Er−O(3) bond lengths range from 2.071(3) to 2.081(2) Å, and the Sm−O(3) bond length in **8** is 2.143(2) Å; these apical Ln−O(3) bonds are all canted (Table 3) from the square-base normal. The Sm−O(3)−C(20) bond angle is 173.1(2)°, and the Er−O(3)−C(20) bond angles range from 172.6(3) to 175.6(1)°. Considering the intense recent interest in rare-earth alkoxide (and chalcogenide) bonding, the Ln^{3+}−O(3) bond lengths in **7**−**10** reside in the "shorter" range of those found in other five-coordinate erbium(III)[22] and samarium(III)[17,24] heteroleptic complexes, and their aforementioned angles are slightly more acute. Although the explanations[17,25] behind these observations remain debatable, agostic interactions between the Ln^{3+} ions and the 2,5-^{t}Bu aryloxide substituent hydrogens are almost certainly not uniquely responsible for this nearly linear Ln−O(3)−C(20) bond (vide infra), and neither complex exhibits noteworthy spectral evidence of Ln···H interactions.

Unlike the (KI)Ln(BHT) complexes, an invariant structure is not expected or observed for the (KI)Ln(N(TMS)$_2$) complexes. A conformation having one methyl from each TMS group close to the apical nitrogen atom would, however, be sterically favorable for the free ligand, and this arrangement is usually observed in its lanthanide complexes. Although the totally eclipsed conformation would possess C_{2v} symmetry, it would simultaneously introduce unfavorable nonbonded methyl···methyl contacts between the two TMS groups. These repulsions are minimized by slight rotation about the Si−N bonds while still leaving one methyl from each TMS (C(25) and C(29), Figure 4), considerably closer to N(3) than the other two methyls. The coordination of such an amido ligand places these two methyl groups over the Ln−O−C−C−C−N− chelate rings near the O···N polyhedral-edge midpoints. Both of these amino methyls protrude further toward the N_2O_2 square and/or Schiff base than the four BHT methyls, which are directed toward the ketoiminato halves (ΔMe in Table 3). Therefore, the amino ligands should produce a more pronounced folding of the Schiff base along the O···N polyhedral edges and/or rotations about the vectors between C(3) or C(9) and the corresponding O···N midpoints. Furthermore, the TMS groups are not locked by the steric volume of the axial ligand near the metal or by the nonbonded contacts with the bridging C(5) and C(7) methylenes. Thus, the amido ligand has more freedom to sample alternate conformations. For example, the entire amido ligand can oscillate about the Ln−N(3) bond while minimizing any methyl−ketoiminato repulsions through a combination of dissymmetric ketoiminato folding or TMS group rotation about the N−Si bonds. This flexibility also allows for greater canting of the Ln−N(3) bond relative to the square-base normal as well as its tipping toward the propyl bridge to give a more accessible metal center for (KI)Ln[N(TMS)$_2$] complexes relative to the corresponding (KI)Ln[BHT] species.

This rotational variability about the Ln−N(3) bond is clearly evident from the plan views (Figure 4) for the two crystallographically independent molecules present in **6**. Even though these two molecules are approximately related in the crystal by a noncrystallographic inversion center at ($^1/_4$, 0, $^1/_4$) in the unit cell, they clearly differ in the extent of rotation about the Ln−N(3) bond. In comparison, the appropriately inverted metal and 15-nonhydrogen atom (vide supra) Schiff-base frameworks for these two crystallographically independent molecules superimpose with a weighted rms deviation

(22) Hitchcock, P. B.; Lappert, M. F.; Singh, A. *J. Chem. Soc., Chem. Commun.* **1983**, 1499.
(23) Clark, D. L.; Gordon, J. C.; Huffman, J. C.; Vincent-Hollis, R. L.; Watkin, J. G.; Zwick, B. D. *Inorg. Chem.* **1994**, *33*, 5903.
(24) Katagiri, K.; Kameoka, M.; Nishiura, M.; Imamoto, T. *Chem. Lett.* **2002**, 426.
(25) Russo, M. R.; Kaltsoyannis, N.; Sella, A. *Chem. Commun.* **2002**, 2458.

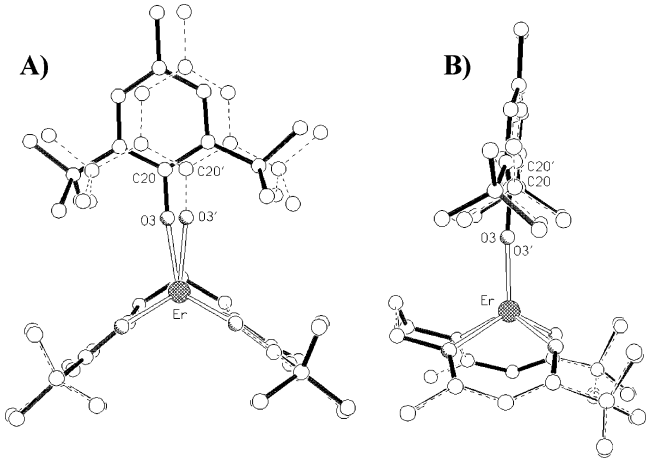

Figure 3. Superimposed enantiomers of complex **7** showing canting of the apical Er−O bond within the phenyl-ring plane.

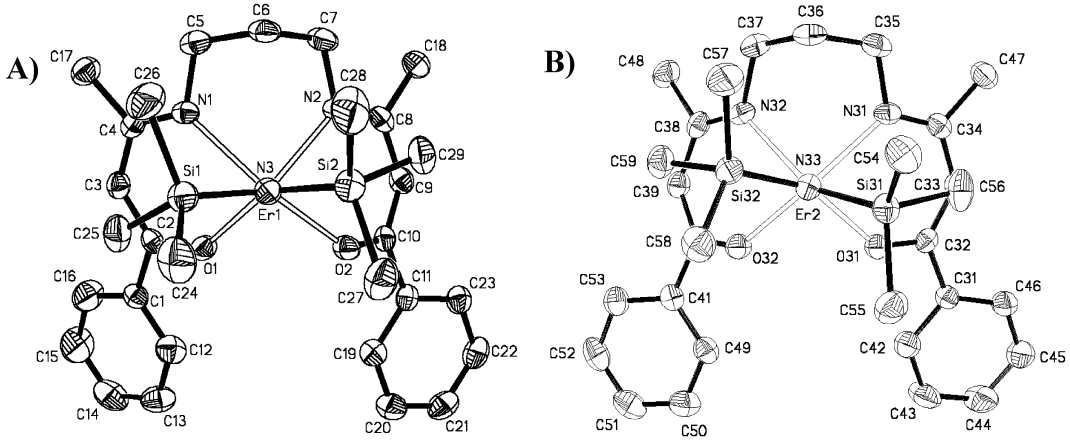

Figure 4. Enantiomers of complex **6** exhibiting Er−N bond twisting.

of 0.30 Å and a N(3)−Er−N(3′) angle of 5.1°. The metal and 15-nonhydrogen atom SB framework for the enantiomer of molecule 1 superimposes with a 0.35-Å rms deviation onto molecule 1 and gives a N_{ap}−Er−$N_{ap'}$ angle of 0°. A similar superposition for the enantiomer of molecule 2 on molecule 1 gives a 0.10-Å rms deviation and a N_{ap}−Er−$N_{ap'}$ angle of 5.0°, which indicates that the steric effects of the apical $N(TMS)_2$ on the Schiff-base distortion are a function of amido ligand tilting and rotation about the amido Ln−N bonds and Si−N bonds.

The structures of **7** and **10** provide a basis for comparing the structural effects of different frontal KI substituents. Both compounds have an apically coordinated, anionic BHT ligand and differ only in the frontal ^{t}Bu (**7**) and Ph (**10**) substituents. The frontal ^{t}Bu substituents have the same rotational restrictions as the BHT ^{t}Bu groups, and they too prefer to have two methyls "straddle" the adjacent carbonyl oxygen with limited rotational freedom about the $^{KI}C-C(CH_3)_3$ bond. The metal and 15-nonhydrogen atom SB framework for the enantiomers of **7** superimposed with a 0.03-Å rms deviation and a 14.1° O_{ap}−Er−$O_{ap'}$ angle, whereas the enantiomers of **10** superimposed (Figure 5) with a 0.40-Å rms deviation and a 13.6° O_{ap}−Er−$O_{ap'}$ angle. It is apparent from Figures 3 and 5 that the Er(KI) fragment differences across the molecular pseudo-mirror plane are almost nonexistent in **7** but become much larger toward the front of the molecule in **10**. Accordingly, **7** exhibits the smallest square-base ruffling (±0.01 Å) when compared to those of **5** and **6** and **8**−**10**, whereas **10** has moderate S_4 ruffling of ±0.14 Å. This can be attributed to four locked ^{t}Bu methyl groups (two pairs on each side of the molecule) buttressed against each other at the front of the molecule in **7** but not in **10** because phenyl groups have replaced the ^{t}Bu groups. The frontal phenyl substituents' orientation is nearly coplanar with the planar ketoiminate halves in our complexes (dissymmetric left to right phenyl−ketoiminato dihedral angles in **10** are 9.1 and 24.1°, respectively) as well as in a recently reported Pd^{2+} dinuclear complex bearing a pentadentate Schiff base derived from the identical diketone.[26] This structural arrangement produces notably short H···H contacts between an ortho hydrogen (on C(16) or C(23)) and the adjacent KI methine hydrogen (on C(3) or C(9)). This is presumably not a sterically imposed conformation but rather is attributable to favorable $\pi-\pi$ interactions between the phenyl ring and the delocalized KI π system. The nearly coplanar arrangement of the phenyl substituents greatly reduces steric crowding at the front of the molecule and is most likely responsible for the observation that complex **10** is an active catalyst for the ring opening of lactides, lactones, and strained epoxides, whereas **7**−**9** fail to react with these monomers.

(26) Mikuriya, M.; Minowa, K.; Lim, J.-W. *Bull. Chem. Soc. Jpn.* **2001**, *74*, 331.

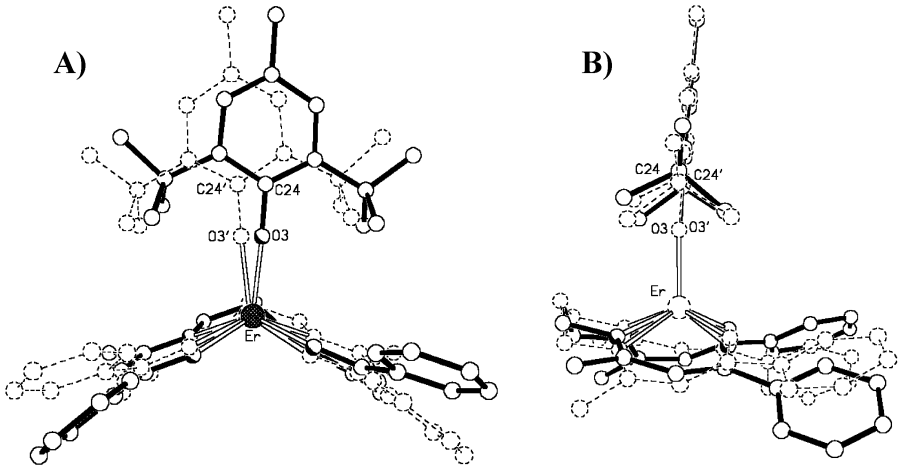

Figure 5. Enantiomers of **10** superposed with a 0.40 Å rms deviation and a 13.6° $O_{ap}-Er-O_{ap'}$ angle. As aryloxide canting occurs, the frontal phenyl substituents rotate to become as coplanar as possible with the planar ketoiminate halves.

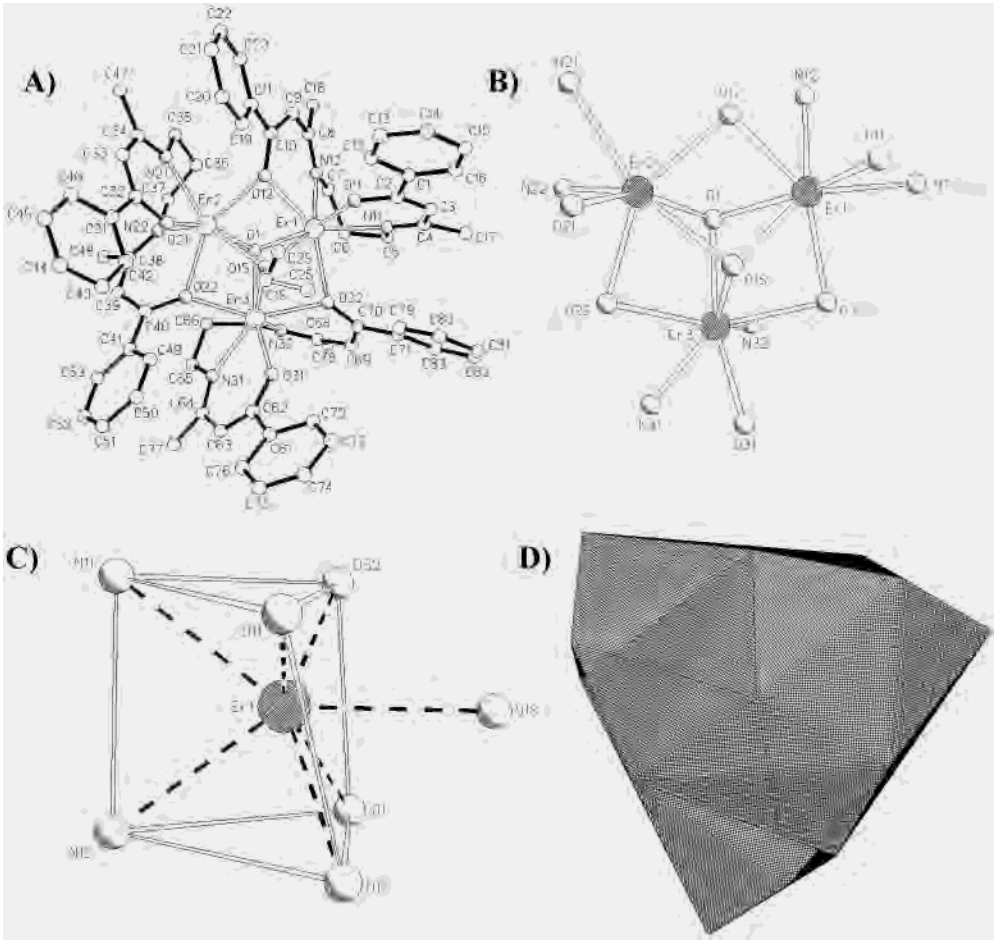

Figure 6. Neutral trimeric Er^{3+} complex **11** (A) with a central core composed of three seven-coordinate Er^{3+} ions bridged by μ_3-oxo, μ_3-alkoxide, and μ_2-O (ketoiminato) linkages (B). Each Er^{3+} ion displays monocapped trigonal prismatic coordination geometry (C), and the individual subunits share capping triangles via O(1)···O(1S) edges in the assembled polyhedra representation (D).

One additional structural feature of alkoxides **7**−**10** needs to be discussed. Tilting of the alkoxide ligands in a plane that is perpendicular to the molecular pseudomirror produces short (≤3.05 Å) Ln···H contacts involving the ortho ^{t}Bu methyl groups (C(27),C(28),C(32),C(33)). Although apical ligand tilting is obvious (Figures 4 and 6), there is no direct spectroscopic evidence for formal M···H interactions with the methyl groups. Nonetheless, Er···H contacts of 2.84 and 3.01 Å persist in **7**. With the methyl hydrogens being positioned as freely rotating rigid rotors with C−H bond lengths of 0.96 Å, these contacts would be shorter if more realistic C−H bond lengths (i.e., longer) were employed and the methyl groups were rotated for maximal Er···H interaction. Even so, the observed 2.84-Å Er···H distance in **7** is only 0.14 Å longer than the standard Er···H distance involving methylene carbon C(6) in **5**−**10**.

Although slightly decreasing ketoiminato frontal steric bulk (^{t}Bu to Ph) still affords mononuclear aryloxide complexes, the stoichiometric alcoholysis of **6** with the significantly smaller ethanol reproducibly yields a neutral trimeric cluster, **11** (Figure 6A), whose central core consists of three seven-coordinate Er^{3+} ions bridged by μ_3-oxo, μ_3-alkoxide, and μ_2-O (ketoiminato) linkages (Figure 6B). The metal ions remarkably serve as the vertices of a nearly perfect equilateral triangle with an edge length of 3.324 (1,7,5,3) Å. Similar, less-ordered dicationic and tricationic species have been reported from aqueous reactions, including $Gd_3(\mu_3\text{-}OH)_2$[27] and $La_3(\mu_3\text{-}OH)(\mu_2\text{-}H_2O)$[28] cores, respectively, as their neutral nitrato salts. The average metrical parameters for the three types of ketoiminato donor atoms in **11**, Er−N, Er−O, and Er−O(μ_2), are 2.428 (3,20,8,6), 2.211 (3,9,6,3), and 2.322 (2,30,19,6) Å, respectively. The average distances of the common Er−O^{2-}(μ_3) and Er−OEt^{1-}(μ_3) are 2.187 (2,6,4,3) and 2.417 (2,20,14,3) Å, respectively. The ethoxide CH_3 terminus is disordered over two positions (modeled at 54 and 46% occupancies) within clefts created by the Schiff-base phenyl groups, all of which reside on a single side of the molecule. The coordination geometry about each Er^{3+} ion is best described as a monocapped trigonal prism[29] (Figure 6C), whose triangular faces are only 1.3° from being parallel. Three of these monocapped trigonal prismatic subunits subsequently assemble with pseudo C_3 symmetry into the trinuclear cluster. Each of these subunits shares a pair of capping triangles having an O(1)···O(1S) edge with adjacent polyhedra (Figure 6B and D). The square face defined by O(1), O(11), O(12), and O(32) exhibits 0.09-Å S_4 ruffling (note: this is not related to the aforementioned discussion of the square planar complexes) with the capping O(1S) atom displaced 1.83 Å from the square mean plane. Synthetically, **11** immediately decomposes upon exposure to the ambient atmosphere (even bathed in Paratone-N), necessitating that the crystals be exclusively handled and mounted at low temperatures in a glovebag.

Initial solution-based homopolymerizations[30] with compounds **1**, **4**−**6**, and **10** and purified ϵ-caprolactone and *rac*-lactide monomers afford biodegradable polyesters. For the amidos, **1** and **4**−**6**, and the alkoxide, **10**, at [monomer]/[catalyst] loads of 150:1 in toluene at 26 and 70 °C for 30 min, high-molecular weight polymers (>92% conversion by ^{1}H NMR and TGA analyses) exhibiting broad polydispersities were recovered. At 26 °C, for both atactic and isotactic lactide polymers, M_n (10^3) varies from 5.3 to 12.6 (tacticity depends on catalyst structure) and exhibits polydispersities from 1.4 to 2.6. At 70 °C, M_n (10^3) ranges from 3.6 to 15.6, again depending on catalyst structure; however, the polydispersities broaden from 4.3 to 6.2. These preliminary observations are attributed to increased chain transfer at higher temperatures, resulting from weaker association of the metal ion and growing polymer chain. For ϵ-caprolactone under similar conditions, M_n (10^3) falls between 33.9 and 38.7 with monomodal polydispersities displaying a narrower range of 2.0 to 3.2. Although these preliminary results establish polymer initiation, a more detailed understanding of the polymerization process, capture of the initiating species, and more controlled polymerizations will be forthcoming.

Summary

This contribution presents the syntheses of mononuclear, anhydrous, solvent-free, five-coordinate lanthanide amido complexes **4**−**6** bearing tetradentate Schiff bases. The Schiff-base ligands are devoid of backbone aromatic groups and contain a C_3H_6 spacer between the ketoiminato halves, providing sufficient N···N separation for larger lanthanide metal capture. Three organic scaffolds, with different front (^{t}Bu and Ph) and rear (*gem*-dimethyl and methylene) steric requirements, all successfully support low coordination numbers (<6) spanning seven contiguous f-element Ln^{3+}. Direct conversion, in high yields and analytical purity, of **1**, **5**, and **6** to bulky aryloxides (**7**−**10**) is accomplished by the stoichiometric reaction with 2,6-bis(*tert*-butyl)-4-methylphenol, without degradation of the N_2O_2 ligand framework but with solvent polymorphism. Attempts to prepare analogous species with a less sterically demanding alcohol, EtOH, reproducibly afforded the neutral trinuclear complex, **11**.

A summary of salient mononuclear amino and alkoxide metrical parameters is given in Tables 2 and 3. The five-coordinate complexes, **5**−**10**, share similarities, including: (1) boat conformation for the six-membered diamine chelate ring that establishes a close contact between the Ln^{3+} ion and a diastereotopic hydrogen on the central C(6) methylene; (2) square pyramidal metal coordination with the Schiff-base donor atoms defining the square base; (3) varying degrees of S_4 ruffling (ΔL) for the square-base donor atoms; and (4) canting ($\angle$ax) of the apical Ln−N(3) or Ln−O(3) bond relative to the normal to this square base. From Table 2, it is clear that the greatest degree of N_2O_2 ruffling and the largest τ values occur for the amido complexes, **5** and **6**; these complexes also have significant asymmetrical folding along the O−N KI edges. This creates innate chirality at the metal center, affording both enantiomers (or racemic pairs) within the crystals and is a result of both KI flexibility and dissymmetric KI···CH_3[$Si(CH_3)_2$] steric repulsions for the two TMS methyl groups (on either side of the idealized σ_v) protruding toward the square base. Conversely, the symmetrical orientation of four aryloxide ^{t}Bu, CH_3 groups downward upon KI C−N and C═O linkages affords more symmetrical ligand folding. Thus, nearly ideal square-pyramidal geometry is observed for the sterically hindered aryloxide complex **7** and its solvent polymorph **9**, despite different solvent-induced packing arrangements.

Complexes **1**, **4**−**6**, and **10** are active initiators for solution-based homopolymerizations of *rac*-lactide and ϵ-caprolactone at temperatures of 26 and 70 °C. Initial experiments provided polymer samples with moderate molecular weights and

(27) Costes, J.-P.; Dahan, F.; Nicodème, F. *Inorg. Chem.* **2001**, *40*, 5285.
(28) Aspinall, H. C.; Black, J.; Dodd, I.; Harding, M. M.; Winkley, S. J. *J. Chem. Soc., Dalton Trans.* **1993**, 709.
(29) Kepert, D. L. *Prog. Inorg. Chem.* **1979**, *25*, 41.
(30) (a) Ovitt, T. M.; Coates, G. W. *J. Am. Chem. Soc.* **2002**, *124*, 1316. (b) Aubrecht, K. B.; Hillmyer, M. A.; Tolman, W. B. *Macromolecules* **2002**, *35*, 644. (c) O'Keefe, B. J.; Monnier, S. M.; Hillmyer, M. A.; Tolman, W. B. *J. Am. Chem. Soc.* **2001**, *123*, 339. (d) Ovitt, T. M.; Coates, G. W. *J. Polym. Sci., Part A: Polym. Chem.* **2000**, *38*, 4686.

polydispersities that broaden at higher temperatures. Under identical conditions, **7**−**9** are completely inactive for the solution polymerization of strained epoxides, lactides, and lactones, presumably because of the monomer's inaccessibility to the metal center. As expected, active polymer initiation accompanies decreased frontal steric bulk (**9** vs **10**).

Acknowledgment. This work was supported by the University of Nebraska Layman Foundation and the Nebraska Research Initiative, and acknowledgment is also made to the donors of the American Chemical Society Petroleum Research Fund for supporting this research. J.A.B. also thanks Professor Eric Fossum of Wright State University for numerous polymerization discussions and for obtaining preliminary GPC data. Dr. Dipanjan Nag of the University of Nebraska—Lincoln is also acknowledged for assistance in obtaining the paramagnetic NMR data presented in this manuscript.

Supporting Information Available: Crystallographic treatment of hydrogen atoms and disordered solvent and thermal ellipsoid plots (where ball-and-stick models are used) and crystallographic files for **4**−**11** in CIF format. This material is available free of charge via the Internet at http://pubs.acs.org. These may also be obtained from the Cambridge Crystallographic Data Center, 12 Union Road, Cambridge, CB2 1EZ, U.K. (fax: +44−1223−336033; e-mail: deposit@ccdc.cam.ac.uk) under assigned CCDC numbers (compound) of 210063 (**4**), 210064 (**5**) 210067 (**6**), 210065 (**7**), 210066 (**8**), 210070 (**9**), 210069 (**10**), and 210068 (**11**).

IC040006F